RSC Advances

RSC Publishing

COMMUNICATION

View Article Online
View Journal | View Issue

High-performance Si anodes with a highly conductive and thermally stable titanium silicide coating layer†

Cite this: *RSC Advances*, 2013, **3**, 2538

Received 19th November 2012,
Accepted 20th December 2012

DOI: 10.1039/c2ra23365g

www.rsc.org/advances

Okji Park, Jung-In Lee, Myung-Jin Chun, Jin-Tak Yeon, Seungmin Yoo, Sinho Choi, Nam-Soon Choi* and Soojin Park*

We report a simple route for synthesizing titanium silicide-coated Si anodes *via* the silicothermic reduction process of TiO_2-coated Si. The titanium silicide enhances the electrical conductivity of Si nanoparticles and provides a highly stable solid electrolyte interface layer during the cycling, resulting in excellent electrochemical performances and significantly improved high thermal stability.

Rechargeable lithium-ion batteries (LIBs) have been developed as the most promising power source technology for portable electronics (*e.g.*, cell phones, laptop computers, digital cameras, *etc.*) and vehicles (*e.g.*, hybrid vehicle, electric vehicle, *etc.*).[1,2] In the last decade, substantial efforts have been devoted to the replacement of conventional carbon-based anode materials in LIBs with alternatives that allow a high energy density.[3–5]

Silicon is an attractive anode material for next-generation LIBs owing to its abundant availability, its low discharge potential (<0.4 V *vs.* Li/Li^+) and high theoretical gravimetric capacity (3579 mAh g^{-1} at room temperature).[6–8] However, the practical use of Si anode material in LIBs is hindered by its poor cyclability resulting from the low intrinsic electrical conductivity and the huge volume change (>300%).[9,10] The use of nanostructured materials is an effective approach to solve this issue. Nanostructured Si anode materials, including nanoparticles,[11,12] nanowires,[4,13,14] nanotubes,[15] hollow spheres,[16] and porous structures,[17,18] showed significantly improved cycle performances by accommodating the large volume change.

An alternative approach for improving the stability of Si is to use surface coating. The surface of an electrode material can greatly influence the electrochemical properties. Considering the potentials at which the Si host alloys with lithium, electrolyte components, especially carbonate esters, will be inevitably reduced into species that are structurally similar to that identified on graphitic anodes.[19] However, fresh Si surfaces are created repeatedly in each cycle and due to the local instability caused by the huge volume change associated with the lithium insertion/extraction process, an additional reduction of electrolytes takes place to cover those newly exposed surfaces. This continuous process consumes the limited Li^+ source, builds up a thick solid electrolyte interface (SEI) layer on the Si active materials, and would eventually disable the cell.[19,20] Therefore, a uniform and compact SEI layer on the electrode surface may enhance the efficiency and cycling stability of the electrode. Typically, carbon-based materials,[21–23] metal particles,[18,24–29] metal oxide particles,[30,31] and conductive polymers[32,33] have been used as coating materials to enhance the electrical conductivity of Si and to form a stable SEI layer, resulting in improved electrochemical performances.

As another simple method, a silicothermic reduction process can provide an attractive means to coat titanium silicide (Ti_xSi_y) on the surface of Si. Since the Ti_xSi_y is light-weight, highly electrically conductive, and thermally stable, when it is combined with Si particles significantly improved electrochemical performances can be expected.[34–36] For example, Zhou *et al.* reported the synthesis of hetero-nanostructures consisting of $TiSi_2$ nanonets and Si nanoparticles *via* a chemical vapor deposition process. The hetero-nanostructured anode materials exhibited remarkable electrochemical performances, including high capacity and long cycling life. However, the amount of inactive $TiSi_2$ should be minimized to make high energy density LIBs.[36]

Herein, we report a simple synthesis of Ti_xSi_y coated Si nanoparticles *via* a silicothermic reduction process, in which Si acts as the reducing agent, while titanium oxide is used as a source material of Ti.‡ The titanium silicide enhances the electrical conductivity of Si nanoparticles and provides a highly stable SEI layer during the cycling, resulting in superior electrochemical performances including a high reversible capacity (1470 mAh g^{-1}) and a high rate capability (1150 mAh g^{-1} at 20 C rate). Moreover, the Ti_xSi_y-coated Si electrodes showed significantly improved high thermal stability, compared to bare Si electrodes.

The synthetic approach of Ti_xSi_y-coated Si nanoparticles is briefly described in the schematic illustration of Fig. 1. We developed a simple wet-chemical synthetic route to evenly coat

Interdisciplinary School of Green Energy, Ulsan National Institute of Science and Technology, Ulsan, Korea 689-798. E-mail: spark@unist.ac.kr; Fax: +82-52-217-2909

† Electronic supplementary information (ESI) available: EDAX profile and XPS spectra of Ti_xSi_y-coated Si particles. See DOI: 10.1039/c2ra23365g

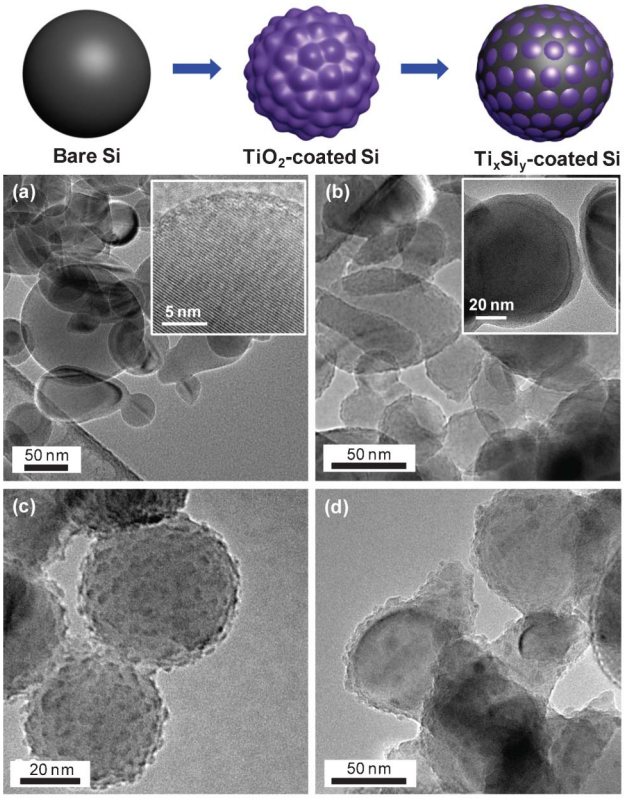

Fig. 1 Synthesis of Ti_xSi_y-coated Si nanoparticles. Top: Schematic illustration preparing Ti_xSi_y layer on the surface of Si particles. Bottom: (a) TEM image of bare Si particles and magnified TEM image (inset of panel a) showing crystalline Si core and SiO_2 shell, (b) TEM image of TiO_2-coated Si particles and magnified image (inset of panel b) showing thickness of TiO_2 layer, (c) TEM image of TiO_2-coated Si particles annealed at 450 °C, and (d) TEM image of Ti_xSi_y-coated Si particles obtained by annealing at 1000 °C.

TiO_2 onto the surface of Si particles by controlled hydrolysis of the titanium precursors. A subsequent two-step annealing process led to the formation of Ti_xSi_y-coated Si particles. A detailed explanation of the synthetic procedures is given in the experimental section.

Fig. 1a presents a transmission electron microscope (TEM) image of Si nanoparticles, showing that the particles consist of a crystalline Si core (ranging from 30 to 100 nm in diameter) and an SiO_2 shell with thickness of ~1 nm (Inset of Fig. 1a). When equal amounts of titanium tetrabutoxide and H_2O were refluxed in a mixture of ethylene glycol/ethanol in the presence of 1 g Si particles, the amorphous TiO_2 precursor was evenly coated on the surface of the Si particles with an average thickness of ~10 nm (Inset of Fig. 1b). The Ti amount of 2.4 wt% was confirmed by inductively coupled plasma mass spectrometry (ICP) analysis. With an increasing Ti precursor, the Ti contents in the final products were linearly increased (Fig. S1, ESI†). The TiO_2 coated Si particles were subsequently annealed at 450 °C for 1 h to prepare TiO_2-decorated Si powders. Consequently, amorphous TiO_2 were transformed to crystalline TiO_2 having an average particle size of 5 nm (Fig. 1c). As the TiO_2-decorated Si particles were further annealed at 1000 °C for 1 h in argon, the TiO_2 was transformed to

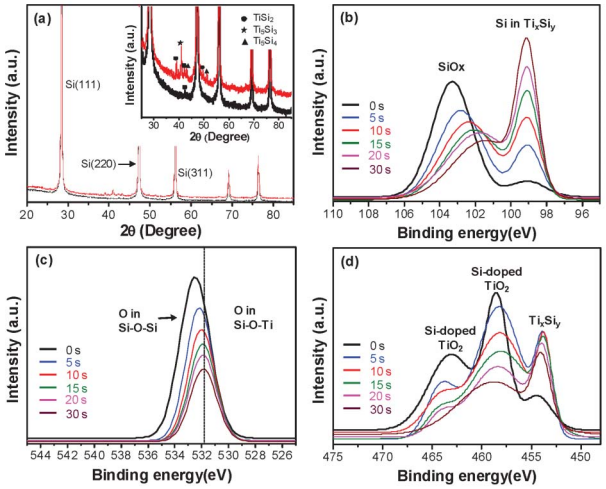

Fig. 2 Characterization of Ti_xSi_y-coated Si nanoparticles. (a) XRD patterns show Ti_xSi_y-coated Si particles annealed at 450 °C (black line) and 1000 °C (red line). In the inset, $TiSi_2$, Ti_5Si_3, and Ti_5Si_4 phases were clearly observed. (b) XPS spectra of the Si 2p core level shows existence of a Ti_xSi_y layer and a formation of Ti–O–Si. XPS depth profiling data indicates the successful synthesis of Ti_xSi_y layers on the surface of Si particles. XPS spectra of (c) O 1s and (d) Ti 2p core levels confirm the formation of strong bonding between Si and TiO_2 (Ti–O–Si) and Ti_xSi_y phases.

Ti_xSi_y *via* a silicothermic reduction process, as will be discussed later (Fig. 1d).

To investigate the formation mechanism of Ti_xSi_y-coated Si particles, we obtained X-ray diffraction (XRD) patterns‡ and X-ray photoelectron spectroscopy (XPS) results. XRD patterns of TiO_2-decorated Si annealed at 450 °C showed that crystalline Si peaks were clearly observed (black line in Fig. 2a), while a weak peak of crystalline $TiSi_2$ phase was detected at 42°, as indicated in the inset of Fig. 2(a). When the annealing temperature was increased to 1000 °C, the intensity of the $TiSi_2$ peak was significantly increased (solid circle in the inset) and a new phase of Ti_5Si_3 (solid star) and Ti_5Si_4 (solid triangle) was developed, (the inset of Fig. 2a). The Ti_5Si_3 and Ti_5Si_4 phases were formed as the $TiSi_2$ phase was further reacted with additional Ti, as marked in the Ti–Si binary phase diagram.[37]

In order to characterize the oxidation states of the silicon, oxygen, and titanium ions, XPS spectra of titanium-silicide coated Si samples were obtained. The structures of the coating layers were investigated through depth profiling by argon ion. The binding energies of Si 2p appearing at 99 eV represent silicon species in the Ti_xSi_y, indicating that Ti_xSi_y-coated Si is successfully synthesized (Fig. 2b). Also, based on the XPS spectra ranging from 103.5 to 101 eV, pure SiO_x exists in the outermost shell and Ti-associated SiO_x in the inner layers was detected with a short time etching, implying that Si–O–Ti bonds may be formed (Fig. 2b).[38] From the binding energy of O 1s appearing at 533 eV (Si–O–Si) and 532 eV (Si–O–Ti), the formation of Si–O–Ti was confirmed, revealing the strong interaction between TiO_2 and Si (Fig. 2c).[39] The XPS spectra of the Ti 2p core level reconfirmed the formation of Si-doped TiO_2 and Ti_xSi_y. In the outermost shell regions, the peaks appearing at 458.5 and 464.3 eV correspond to the core level of Ti 2p of TiO_2. Ti

2p peaks corresponding to the Si-dope TiO_2 and the Ti_xSi_y were gradually increased through deep depth profiling (Fig. 2d).[40]

The formation of Ti_xSi_y layers can be described as follows: (i) When the TiO_2 coating layers were heated to >900 °C, the dissociation of TiO_2 is fast, leaving oxygen vacancies;[41] (ii) At the same temperature, Si atoms easily diffuse into the dissociated and remaining TiO_2 layers to make $TiSi_2$ layers; (iii) The little remaining oxygen may react with the Si to make SiO at the shell regions, in which the SiO will be evaporated at >900 °C; (iv) Finally, the Ti_5Si_3 and Ti_5Si_4 phases are formed by the reaction of the preformed $TiSi_2$ phase and additional dissociated Ti. The overall reaction to form Ti_xSi_y is denoted in the following equations:[42]

$$Ti + 2Si \rightarrow TiSi_2 \quad (1)$$

$$TiO_2 + 4Si \rightarrow TiSi_2 + 2SiO \uparrow \ (>900\ ^\circ C) \quad (2)$$

$$yTiSi_2 + (2x - y)Ti \rightarrow 2Ti_xSi_y \quad (3)$$

The electrochemical performance of the Ti_xSi_y-coated Si particles‡ (Ti contents of 2.3 wt%) as the anodes in LIBs was tested by galvanostatic discharging and charging at a 0.1–20 C rate in the range of 0.005 V to 1.2 V. The first discharge and charge capacity of bare Si at a 0.1 C rate are 1950 and 1550 mAh g^{-1}, corresponding to a coulombic efficiency of 79.4% (Fig. 3a). Whereas, the first charge capacity of the Ti_xSi_y-coated Si at a 0.1 C rate is 1470 mAh g^{-1} with an increased coulombic efficiency of 83.5% (Fig. 3b). The enhanced coulombic efficiency of the first cycle may be due to the uniform Ti_xSi_y coating layer, which can maintain a SEI layer on the surface of the Si particles and reduce the direct contact between Si and the electrolyte.

When the Ti_xSi_y-coated Si electrode was cycled to 90 cycles at a rate of 0.2 C (lithiation) and 0.5 C (delithiation), a high reversible capacity of 1430 mAh g^{-1} was exhibited, corresponding to the capacity retention of >99% (compared to initial capacity) (Fig. 3c). In contrast, the bare Si electrode showed a fast capacity fading with capacity retention of 51% after 70 cycles (Fig. 3c). It is attributed to poor electrical conductivity and the formation of an unstable SEI layer.[7] Cross–sectional SEM images of bare and Ti_xSi_y-coated Si showed the thickness of the electrodes before and after cycling. The bare Si electrode showed the volume expansion of 62.3%, while the Ti_xSi_y-coated Si exhibited less volume expansion (30%) due to the coating effect and the stable SEI layer (Fig. S2, ESI†).

Moreover, rate capabilities of both electrodes were investigated at various C rates (0.2–20 C rate) between 1.2 V and 0.005 V with a fixed discharging rate of 0.2 C. The bare Si electrodes exhibited the capacity retention of 66.7% at a high rate of 10 C, compared to that of the 0.2 C rate (Fig. 3d). In contrast, the Ti_xSi_y-coated Si electrode showed significantly enhanced rate capabilities. Even at a high rate of 20 C, the capacity retention of the Ti_xSi_y-coated Si was 87.8% (Fig. 3d). These results suggest that the Ti_xSi_y coating layers play an important role in exhibiting superior electrochemical properties, including highly stable cycling and an excellent rate capability. Since the Ti_xSi_y layers were strongly attached to the Si interface during the silicothermic reduction process, the Ti_xSi_y-coated Si electrodes may exhibit a highly stable cycling. Moreover, the electrical conductivity of the electrodes prepared with bare Si was 4.23×10^{-5} S cm^{-1}, while the Ti_xSi_y-coated Si electrode showed a significant improvement (1.87×10^{-4} S cm^{-1}), indicating that the Ti_xSi_y layer served as the effective path for electrical conduction.

To prove the stable cycling of Ti_xSi_y-coated Si electrodes, the XPS spectra were obtained before and after cycling. Interestingly, the SEI layer did not discernibly change between the 1st and 40th cycles, supporting good capacity retention of the Si anodes with the Ti_xSi_y coating layer (Fig. S3 and S4, ESI†).

In addition, the effect of the Ti_xSi_y coating on the thermal properties of the fully lithiated Si electrode was investigated by differential scanning calorimetry (DSC).‡ Heating of the fully lithiated bare Si electrode resulted in distinct and sharp exothermic peaks at around 107, 187, 251, and 262 °C (Top in Fig. 4a). It is reasonable that the first exothermic peaks at 100–130 °C correspond to thermal decomposition of metastable SEI components.[43] Heat evolution (55 J g^{-1}) for the first exothermic peak of the fully lithiated Ti_xSi_y-coated Si was larger than that of fully lithiated bare Si (37 J g^{-1}) in the presence of an electrolyte. In order to clarify this point, the XPS analysis of the SEI on bare and Ti_xSi_y-coated Si electrodes was performed. From the XPS results, it is clearly seen that a $LiPF_6$ salt, which is thermally unstable and highly reactive with trace water, is trapped in the SEI on the coated Si after 1 cycle (Fig. S3, ESI†). It should be noted that PF_5 formed from $LiPF_6$ decomposes to POF_3 in the presence of water traces (in an electrolyte and an electrode) and the reactive POF_3 in the electrolyte reacts with carbonate solvents, such as EC and DEC to produce CO_2 and OPF_2ORF at elevated temperatures, as illustrated in the ESI (Fig. S5, ESI†). This kind of reaction may generate additional exothermic heat and results in augmentation of heat evolution for the first exothermic peak of the fully lithiated Ti_xSi_y-coated Si.

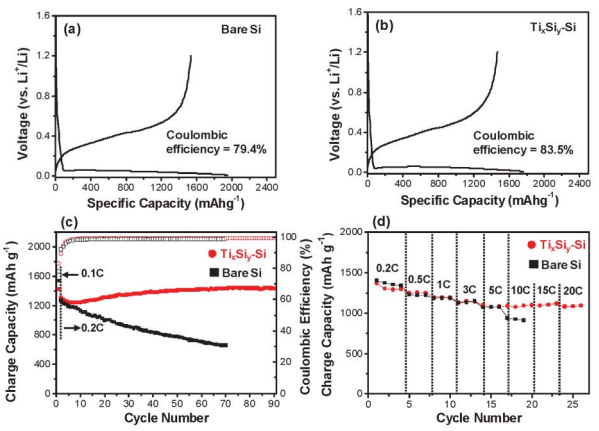

Fig. 3 Electrochemical performances of Ti_xSi_y-coated Si and bare Si anodes. First cycle voltage profiles of (a) bare Si and (b) Ti_xSi_y-coated Si are obtained at 0.1 C (1st cycle) in the range of 0.005–1.2 V. (c) Cycling performances of both electrodes are obtained at 0.1 C (first cycle) and 0.2 C (from second cycle). (d) Rate capabilities of Ti_xSi_y-coated Si (solid circle) and bare Si (solid square) were obtained at 0.2 C–20 C rates.

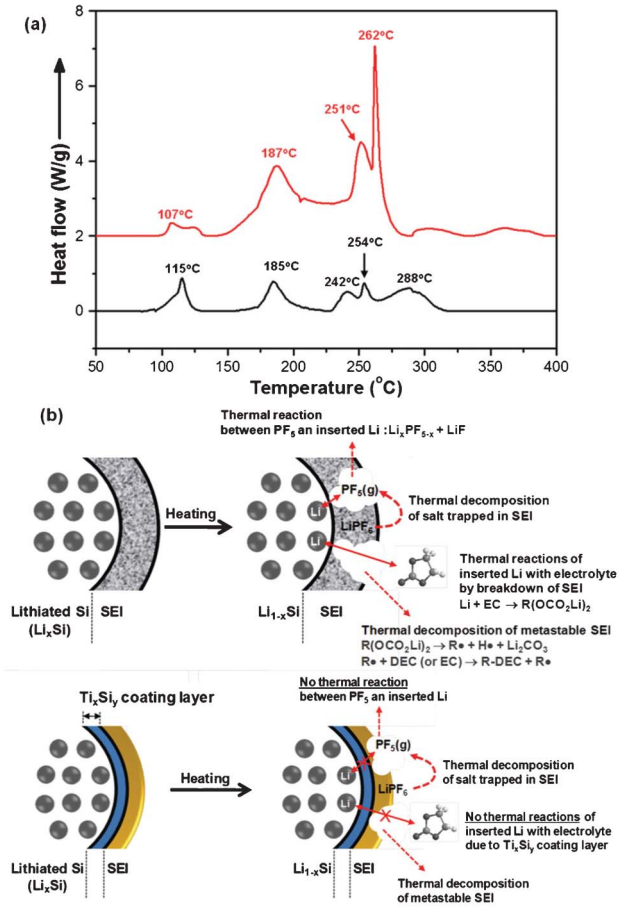

Fig. 4 Thermal stability of bare Si and Ti_xSi_y-coated Si electrodes. (a) DSC profiles of bare Si and Ti_xSi_y-coated Si electrodes. (b) Schematic illustration showing the thermal decomposition reactions of an electrolyte with lithiated Si at elevated temperatures.

A DSC heating curve for fully lithiated bare Si shows very large exothermic peaks at 150–320 °C, while the presence of the Ti_xSi_y coating layer on fully lithiated Si gives broad exothermic peaks with significantly reduced heat (Bottom in Fig. 4a). It indicates that the Ti_xSi_y coating layer effectively mitigated various exothermic reactions caused by the thermal decomposition reactions of an electrolyte with lithiated Si at elevated temperatures, as depicted in Fig. 4(b). When a cell is heated above a certain temperature, exothermic reactions between the electrodes and the electrolyte take place and leads to an increase of the internal cell temperature. If the generated heat is greater than the energy that can be dissipated, the cell temperature will increase rapidly. This temperature growth will accelerate chemical reactions and lead to the production of even more heat, eventually resulting in the thermal runaway of batteries. From this point of view, it can be expected that the Ti_xSi_y coating layer on Si anode materials improves battery safety because the exothermic heat evolution (324 J g^{-1}) in the overall 80–320 °C was greatly reduced compared to non-coated Si electrodes (912 J g^{-1}).

Conclusions

We successfully synthesized titanium silicide coated silicon particles *via* a silicothermic reduction process of Si and TiO_2. The TiO_2 layers were evenly coated on the surface of Si in a solution, and subsequent thermal annealing led to the formation of titanium silicide coated Si particles. Since titanium silicide are electrically conductive and form a highly stable SEI layer, Ti_xSi_y-coated Si electrodes exhibit high electrochemical performances, including a high specific capacity and an excellent rate capability. Also, the Ti_xSi_y-coated Si electrodes showed significantly improved thermal stability, compared to non-coated Si electrodes. This process opens up a way to make other silicon-based anode materials for high performance lithium-ion batteries.

Acknowledgements

This work was supported by the MKE/ITRC program of NIPA (NIPA-2012-C1090-1200-0002) and the Conversing Research Center Program through the Ministry of Education, Science and Technology (2011K000637).

Notes and references

‡ *Preparation of Ti_xSi_y-coated Si particles*: Si nanopowder (Sigma-Aldrich, 50 nm in size) was cleaned in acetone and isopropyl alcohol and dried under nitrogen. In a typical synthesis, 0.2 mL of titanium tetrabutoxide and 0.2 mL of H_2O were refluxed in ethylene glycol/ethanol (16 mL/4 mL) at 80 °C for 6 h in the presence of 1 g Si particles. As-synthesized TiO_2-coated Si powders were cleaned with ethanol several times and dried at 80 °C for 12 h. Subsequently, the TiO_2-coated Si particles were thermally annealed in a quartz furnace at 450–1000 °C for 1 h under argon stream to make Ti_xSi_y-coated Si particles.

Characterization of Ti_xSi_y-coated Si particles: The crystal structures of the Ti_xSi_y-coated Si sample were measured by a high power X-ray diffractometer (XRD) on a Rigaku D/MAX at 2500 V using Ni-filtered Cu-Kα radiation. TEM images were taken in the bright-field mode using JEM 1400 (JEOL) operated at 120 kV accelerating voltages.

Thermal analyses of lithiated Ti_xSi_y-coated Si particles: To measure the thermal properties of lithiated Si electrodes with electrolytes, coin cells were charged to 0.005 V *vs.* Li/Li^+ and then carefully opened in a dry room. The retrieved electrodes were rinsed in a DMC solvent to remove residual electrolyte and then dried. The resulting lithiated silicon electrode was sealed together with an electrolyte in a hermetic stainless-steel pan (Perkin Elmer). All of the DSC (METTLER TOLEDO DSC 1) measurements were carried out at a heating rate of 5 °C min^{-1} in a range of 30–400 °C. The amount of entrapped electrolyte was 50 wt% based on the lithiated silicon material.

Electrochemical performance: An electrochemical cell test was performed using coin-type half cells (2016R type) by assembly in an argon-filled glove box. Ti_xSi_y-coated Si and bare Si electrodes for the cell test were composed of Si active material (70 wt%), super P carbon black (10 wt%), and poly(acrylic acid)/sodium carboxymethyl cellulose (wt/wt, 50/50) binder (20 wt%). The electrolyte was composed of 1.3 M $LiPF_6$ in a mixture of ethylene carbonate/diethylene carbonate (ED/DEC, 30/70 vol.%) with 5 wt% fluoroethylene carbonate (FEC) additive. The cells were cycled at a rate of 0.1–20 C in the range of 0.005 and 1.2 V.

1 J. M. Tarascon and M. Armand, *Nature*, 2001, **414**, 359.
2 P. G. Bruce, B. Scrosati and J.-M. Tarascon, *Angew. Chem., Int. Ed.*, 2008, **47**, 2930.
3 M. S. Whittingham, *Chem. Rev.*, 2004, **104**, 4271.
4 C. K. Chan, H. Peng, G. Liu, K. McIlwrath, X. F. Zhang, R. A. Huggins and Y. Cui, *Nat. Nanotechnol.*, 2008, **3**, 31.
5 A. Magasinski, P. Dixon, B. Herzberg, A. Kvit, J. Ayala and G. Yushin, *Nat. Mater.*, 2010, **9**, 353.

6 T. D. Hatchard and J. R. Dahn, *J. Electrochem. Soc.*, 2004, **151**, A838.
7 M. N. Obrovac and L. J. Krause, *J. Electrochem. Soc.*, 2007, **154**, A103.
8 X. H. Liu, L. Q. Zhang, L. Zhong, Y. Liu, H. Zheng, J. W. Wang, J. H. Cho, S. A. Dayeh, S. T. Picraux, J. P. Sullivan, S. X. Mao, Z. Z. Ye and J. Y. Huang, *Nano Lett.*, 2011, **11**, 2251.
9 U. Kasavajjula, C. Wang and A. J. Appleby, *J. Power Sources*, 2007, **163**, 1003.
10 H. Li, Z. X. Wang, L. Chen and X. J. Huang, *Adv. Mater.*, 2009, **21**, 4593.
11 Y. S. Hu, R. Demir-Cakan, M.-M. Titirici, J. O. Muller, R. Schlogl, M. Antonietti and J. Maier, *Angew. Chem., Int. Ed.*, 2008, **47**, 1645.
12 P. F. Gao, J. W. Fu, J. Yang, R. G. Lu, J. L. Wang and X. Z. Tang, *Phys. Chem. Chem. Phys.*, 2009, **11**, 11101.
13 W. Wang and P. N. Kumta, *ACS Nano*, 2010, **4**, 2233.
14 B. M. Bang, H. Kim, J.-P. Lee, J. Cho and S. Park, *Energy Environ. Sci.*, 2011, **4**, 3395.
15 M.-H. Park, M. G. Kim, J. Joo, K. Kim, J. Kim, S. Ahn, Y. Cui and J. Cho, *Nano Lett.*, 2009, **9**, 3844.
16 H. Ma, F. Cheng, J. Chen, J. Zhao, C. Li, Z. Tao and J. Liang, *Adv. Mater.*, 2007, **19**, 4067.
17 H. Kim, B. Han, J. Choo and J. Cho, *Angew. Chem., Int. Ed.*, 2008, **47**, 10151.
18 Y. Yu, L. Gu, C. Zhu, S. Tsukimoto, P. A. van Aken and J. Maier, *Adv. Mater.*, 2010, **22**, 2247.
19 K. Wu and A. von Cresce, *J. Mater. Chem.*, 2011, **21**, 9849.
20 Q. M. Pan, H. B. Wang and Y. H. Jiang, *Electrochem. Commun.*, 2007, **9**, 754.
21 H. Yoo, J.-I. Lee, H. Kim, J.-P. Lee, J. Cho and S. Park, *Nano Lett.*, 2011, **11**, 4324.
22 L. F. Cui, Y. Yang, C. M. Hsu and Y. Cui, *Nano Lett.*, 2009, **9**, 3370.
23 Y. S. Hu, P. Adelhelm, B. M. Smarsly and J. Maier, *ChemSusChem*, 2010, **3**, 231.
24 S. Murugesan, J. T. Harris, B. A. Korgel and K. J. Stevenson, *Chem. Mater.*, 2012, **24**, 1306.
25 Y. L. Kim, H. Y. Lee, S. W. Jang, S. H. Lim, S. J. Lee, H. K. Baik, Y. S. Yoon and S. M. Lee, *Electrochim. Acta*, 2003, **48**, 2593.
26 X. L. Yang, Z. Y. Wen, S. H. Huang, X. J. Zhu and X. F. Zhang, *Solid State Ionics*, 2006, **177**, 2807.
27 J. B. Kim, H. Y. Lee, K. S. Lee, S. H. Lim and S. M. Lee, *Electrochem. Commun.*, 2003, **5**, 544.
28 J. W. Kim, J. H. Ryu, K. T. Lee and S. M. Oh, *J. Power Sources*, 2005, **147**, 227.
29 D. C. Johnson, J. M. Mosby, S. C. Riha and A. L. Prieto, *J. Mater. Chem.*, 2010, **20**, 1993.
30 Y. He, X. Yu, Y. Wang, H. Li and X. Huang, *Adv. Mater.*, 2011, **23**, 4938.
31 H. Wu, G. Chan, J. W. Choi, I. Ryu, Y. Yao, M. T. McDowell, S. W. Lee, A. Jackson, Y. Yang, L. Hu and Y. Cui, *Nat. Nanotechnol.*, 2012, **7**, 310.
32 Y. Yao, N. Liu, M. T. McDowell, M. Pasta and Y. Cui, *Energy Environ. Sci.*, 2012, **5**, 7927.
33 Z. P. GuO, J. Z. Wang, H. K. Liu and S. X. Dou, *J. Power Sources*, 2005, **146**, 448.
34 R. W. Mann, L. A. Clevenger, P. D. Agnello and F. R. White, *IBM J. Res. Dev.*, 1995, **39**, 403.
35 Z. Ma, L. H. Allen and D. D. J. Allman, *Appl. Phys. Lett.*, 1995, **77**, 4383.
36 S. Zhou, X. Liu and D. Wang, *Nano Lett.*, 2010, **10**, 860.
37 T. B. Massalsky, *Binary Alloy Phase Diagram*, ASM, 1990, p.3370.
38 Z. Jiang, X. Dai and H. Middleton, *Mater. Sci. Eng., B*, 2011, **176**, 79.
39 P. M. Kumar, S. Badrinarayanan and M. Sastry, *Thin Solid Films*, 2000, **358**, 122.
40 G. B. Song, H. Joly, F. S. Liu, T. J. Peng, P. Wan and J. K. Liang, *Appl. Surf. Sci.*, 2003, **220**, 159.
41 M. Berti, A. V. Drigo, C. Cohen, J. Siejka, G. G. Bentini, R. Nipoti and S. Guerri, *J. Appl. Phys.*, 1984, **55**, 3558.
42 F. Zhao, X. Cui, B. Wang and J. G. Hou, *Appl. Surf. Sci.*, 2006, **253**, 2785.
43 N.-S. Choi, I. A. Profatilova, S.-S. Kim and E.-H. Song, *Thermochim. Acta*, 2008, **480**, 10.

